Published in final edited form as:
Acta Biomater. 2013 May ; 9(5): 6393–6402. doi:10.1016/j.actbio.2013.01.016.

Biomaterial-Mediated Delivery of Degradative Enzymes to Improve Meniscus Integration and Repair

Feini Qu, BSE[1,2,3,4], **Jung-Ming G. Lin, BS**[1,2], **John L. Esterhai, MD**[1,3], **Matthew B. Fisher, PhD**[1,3], and **Robert L. Mauck, PhD**[1,2,3,*]

[1]McKay Orthopaedic Research Laboratory, Department of Orthopaedic Surgery, Perelman School of Medicine, University of Pennsylvania, Philadelphia, PA 19104, USA

[2]Department of Bioengineering, School of Engineering and Applied Science, University of Pennsylvania, Philadelphia, PA 19104, USA

[3]Philadelphia Veterans Administration Medical Center, Philadelphia, PA 19104, USA

[4]School of Veterinary Medicine, University of Pennsylvania, Philadelphia, PA 19104, USA

Abstract

Endogenous repair of fibrous connective tissues is limited, and there exist few successful strategies to improve healing after injury. As such, new methods that advance repair by promoting cell growth, extracellular matrix (ECM) production, and tissue integration would represent a marked clinical advance. Using the meniscus as a test platform, we sought to develop an enzyme-releasing scaffold that enhances integrative repair. We hypothesized that the high ECM density and low cellularity present physical and biologic barriers to endogenous healing, and that localized collagenase treatment might expedite cell migration to the wound edge and tissue remodeling. To test this hypothesis, we fabricated a delivery system in which collagenase was stored inside electrospun poly(ethylene oxide) (PEO) nanofibers and released upon hydration. *In vitro* results showed that partial digestion of the wound interface improved repair by creating a microenvironment that facilitated cell migration, proliferation, and matrix deposition. Specifically, treatment with high-dose collagenase led to a 2-fold increase in cell density at the wound margin and a 2-fold increase in integrative tissue compared to untreated controls at 4 weeks ($p \leq 0.05$). Furthermore, when composite scaffolds containing both collagenase-releasing and structural fiber fractions were placed inside meniscal tears *in vitro*, enzyme release acted locally and resulted in a positive cellular response similar to that of global treatment with aqueous collagenase. This innovative approach of targeted enzyme delivery may aid the many patients that exhibit meniscal tears by promoting integration of the defect, thereby circumventing the pathologic consequences of partial meniscus removal, and may find widespread application in the treatment of injuries to a variety of dense connective tissues.

[*]**Corresponding Author**: Associate Professor of Orthopaedic Surgery and Bioengineering McKay Orthopaedic Research Laboratory Department of Orthopaedic Surgery Perelman School of Medicine University of Pennsylvania 36th Street and Hamilton Walk Philadelphia, PA 19104 Phone: (215) 898-3294 Fax: (215) 573-2133 lemauck@mail.med.upenn.edu.

Disclosures No disclosures or conflicts of interest.

Keywords

drug delivery; enzyme; meniscus tear; nanofibrous scaffold; wound healing

1. Introduction

Fibrous dense connective tissues of the musculoskeletal system, including the knee meniscus, the temporomandibular menisci, the annulus fibrous of the intervertebral disc, and tendons and ligaments, are characterized by an extracellular matrix (ECM) composed of aligned type I collagen bundles. This fiber-reinforced microstructure gives rise to anisotropic mechanical properties, permitting resistance to tensile stresses applied along the fiber direction. In the knee meniscus, a semilunar fibrocartilaginous structure located between the femur and tibia, circumferentially arranged collagen fibers resist tensile hoop stresses that arise with joint loading [1]. Meniscal tears are common, accounting for over 1 million surgical procedures each year in the United States [2]. These tears disrupt the essential collagen architecture of the meniscus, decreasing its load transfer functionality. The intrinsic healing capacity of this tissue is very poor, especially in avascular regions. Even if some healing occurs, it does so through the formation of a disorganized scar tissue, altering joint biomechanics and eventually leading to degenerative osteoarthritis of the affected knee compartment [3-5].

While multiple repair techniques have been developed, their success is limited to simple longitudinal tears that occur in the vascularized, peripheral one-third of the meniscus [6]. Indeed, a postoperative evaluation of arthroscopically repaired avascular meniscal tears reported that up to 75% of repairs had failed to heal completely, with 20% requiring a secondary surgery [7]. The standard surgical treatment after repair failure is a partial meniscectomy [5], although many surgeons will perform this procedure as a first line treatment option given the poor outcomes for most repair scenarios. However, resection of the damaged portion provides only temporary alleviation of pain, and long-term consequences include increased peak pressures on the tibial plateau during loading, resulting in further degeneration of both the meniscal fibrocartilage and articular cartilage and often culminating in the need for total knee arthroplasty [8, 9].

An ideal alternative to surgical removal would be to reestablish native tissue function by enhancing surgical repair and promoting cell growth, organized ECM production, and, most importantly, integration at the wound site via the creation of an instructive regenerative microenvironment. Experimental strategies to augment connective tissue repair, specifically the avascular zone of the meniscus and other fibrous tissues, include enhancing blood supply via vascular access channels or synovial flaps [10, 11], delivering growth factors to promote neovascularization, cell proliferation, and matrix synthesis [12-15], and provision of synthetic scaffolds that fill the tissue defect [16-19]. A number of factors play a role in successful meniscal repair, including control of the inflammatory state [20], provision of local vascularity [5, 21], and tissue maturity and matrix density [22]. Immature fibrous tissues such as meniscus [22], tendon [23], and ligament [24] show enhanced healing capacity compared to mature tissues, owing to their hypervascular and hypercellular state. Notably, collagen content and diameter increase with developmental stage and skeletal maturation, while cellularity decreases markedly [25]. Furthermore, while the biologic environment may favor regenerative healing of immature tissue, it has recently been shown that fetal sheep tendon undergoes a robust healing response even when transplanted to an adult *in vivo* setting [26], suggesting innate differences mediate the different healing capacity as a function of developmental state.

In agreement with this body of literature, our previous work on meniscus healing *in vitro* suggests that the high ECM density of the mature meniscus represents a physical barrier to endogenous healing [22], where matrix density acts to limit cell proliferation, migration, and matrix remodeling at or near the wound site, leading to an inferior repair response. In contrast to a two-dimensional environment, cells in tissues must overcome the biophysical resistance imparted by their surroundings, and a dense matrix with low porosity and degradability will obstruct cellular movement and activity [27, 28]. Indeed, a number of studies have demonstrated that treatment of the wound edge with matrix-degrading enzymes, including trypsin, collagenase, and hyaluronidase, can enhance articular cartilage graft integration [29-31].

To render this technology clinically feasible, enzymatic degradation must be conducted in a controlled and targeted manner to localize digestion to the wound site. One potential delivery vehicle is nanofibrous scaffolds fabricated via electrospinning. In this well-established process, fibers that are hundreds of nanometers in diameter can be formed and compiled into a non-woven 3D scaffold. Fibers within the scaffold can be collected to resemble the organized collagen bundles found in many fibrous connective tissues. Previously, we have shown that mesenchymal stem cells cultured on aligned poly(ε-caprolactone) (PCL) nanofiber scaffolds organize and deposit collagen along the fiber direction, producing meniscus-like engineered constructs that increase in mechanical properties with time in culture [32]. Furthermore, composites with multiple fiber populations can be formed with differing degradative characteristics in each fiber fraction. For instance, inclusion of water-soluble poly(ethylene oxide) (PEO) fibers into such composites increased scaffold pore size upon hydration and expedited cellular infiltration and tissue maturation [16, 33, 34]. These ‘sacrificial’ fibers can be modified to entrap drug-delivering microspheres [35], where release is dependent on microsphere composition, or directly liberate biologic factors into an aqueous environment [36].

With such regenerative tools at hand, our goal was to develop a functionalized scaffold to enhance meniscal repair. We hypothesized that the high ECM density of the native adult meniscus impedes healing and that decreasing the matrix density may improve cell migration, division, and matrix deposition for integrative repair. To test this hypothesis, we used an *in vitro* explant model to show that partial degradation of the wound edge can alter the structure of adult meniscus, and demonstrated that this treatment improves cellularity and production of new contiguous tissue spanning the wound site. More importantly, we developed a novel method to deliver a controlled, low dose of matrix-degrading enzyme via electrospun composite nanofibrous scaffolds, where the sacrificial PEO component released a single localized dose of collagenase.

2. Materials and Methods

2.1 Preparation and Culture of Meniscus Repair Constructs

Menisci from fetal (mid-gestation) and adult (skeletally mature) cows were sterilely dissected and the synovium removed. Tissue cylinders were excised with an 8 mm biopsy punch and concentrically cored with a 4 mm punch. In a first study, samples were incubated in basal media (BM; Dulbecco’s Modified Eagle’s Medium with 10% Fetal Bovine Serum and 1% Penicillin/Streptomycin/Fungizone) supplemented with 0.05 mg/mL collagenase (type IV from *Clostridium histolyticum*, ≥125 collagenase digestion units/mg solid, Sigma-Aldrich, St. Louis, MO) at 37°C for 6 hours, after which the cores were replaced within the annuli. Controls were incubated in BM only. Repair constructs were cultured in a chemically-defined medium (high glucose DMEM with 1% PSF, 0.1 mM dexamethasone, 50 mg/mL ascorbate 2-phosphate, 40 mg/mL L-proline, 100 mg/mL sodium pyruvate, 1X ITS (6.25 mg/mL Insulin, 6.25 mg/mL Transferrin, 6.25 ng/mL Selenous Acid, 1.25 mg/mL

Bovine Serum Albumin, and 5.35 mg/mL Linoleic Acid) with 10 ng/mL TGF-β3) for 4 weeks in non-tissue culture treated 6-well plates. To investigate the long-term effect of collagenase pre-treatment, adult meniscus cores and annuli were incubated with 0 (BM), 0.01 (LC; low-dose collagenase), or 0.05 mg/mL (HC; high-dose collagenase) collagenase, reassembled into repair constructs, and cultured for 1, 4, or 8 weeks as above.

2.2 Histological, Biochemical, and MicroCT Analysis of Repair Constructs

At set intervals, repair constructs were fixed in 4% paraformaldehyde, embedded in paraffin, and axially sectioned to 8 μm thickness onto glass slides. Sections were stained with Hematoxylin and Eosin (H&E), Picrosirius Red (PSR), and 4',6-diamidino-2-phenylindole (DAPI, Prolong Gold; Invitrogen, Grand Island, NY) to visualize ECM density, collagen, and cell nuclei, respectively. Quantitative parameters of integration were derived from histological sections. Percent integration was defined as the cumulative distance of annulus-to-core contact normalized by the core perimeter (n=3-4/group). Cell density at the interface was determined by counting the number of nuclei present within 100 μm of the interface using ImageJ (Wayne Rasband, NIH) (n=4/group). DNA content was biochemically assessed in both the core and annulus at each time point in additional constructs (n=6-7/group). Tissue segments were weighed separately, lyophilized, and reweighed to determine water content. Following digestion in a buffer containing 2% papain at 60°C, DNA content per dry weight was determined via the PicoGreen assay (Invitrogen). Lastly, constructs from each group were saturated in Lugol's contrast solution (Sigma-Aldrich) for 24 hours and scanned via microcomputed tomography at an energy level of 70 kV and intensity of 114 μA (μCT; ScanCo, VivaCT 70, Wayne, PA) to assess matrix changes at the interface (n=4/group).

2.3 Fabrication and Characterization of Enzyme-Releasing Nanofibers

To fabricate enzyme-releasing nanofibers, a solution of 8% w/v PEO (200 kD, Polysciences, Warrington, PA) was prepared in 1:1 EtOH and distilled H_2O with 0.85% w/v NaCl or 2.5% w/v trypsin in the same solution (Invitrogen). These solutions were electrospun onto glass cover slips for 10-15 minutes using a custom device [33]. The spinneret was charged to 15 kV and the polymer flow rate was set at 1.6 mL/hour to produce a stable electrospinning jet. Formed nanofibers were sputter coated with AuPd and imaged via scanning electron microscopy (SEM; Philips XL 20, SEMTech, North Billerica, MA) operating at an accelerating voltage of 10 kV. Fiber diameter was measured using ImageJ (n=100/group).

To determine whether enzyme activity was preserved through the electrospinning process, both cell- and tissue-based assays were employed. Using a cell-based approach, approximately 0.2 and 0.4 g of each fiber type (PEO only or PEO-trypsin) were hydrated in 4 mL of Hank's Buffered Salt Solution (HBSS; Invitrogen) on an orbital shaker for 20 minutes. Confluent monolayers of bovine mesenchymal stem cells (bMSCs, isolated as in [32]) were exposed to these eluted solutions. Four experimental conditions were tested: BM, HBSS, HBSS containing hydrated PEO fibers (PEO), and HBSS containing hydrated PEO-trypsin fibers (PEO-T). A standard solution of trypsin (Invitrogen) at 0.25% w/v in HBSS was used as a positive control. bMSCs were maintained at 37°C in a standard tissue culture incubator with images captured every 10-20 minutes with a light microscope (n=2/group). Solutions were aspirated after 60 minutes for final imaging. Cells were re-plated and cultured for 24 hours to ensure that cells remained viable after treatment.

To further demonstrate efficacy and dosage of delivered trypsin, cylindrical articular cartilage samples were sterilely isolated using 4 mm biopsy punches from the trochlear groove of juvenile bovine femurs and trimmed to a height of 3 mm. Solutions containing hydrated PEO or PEO-trypsin nanofibers (0.4 g) were incubated with the cartilage cylinders

for 3 and 6 hours, along with BM and HBSS controls. HBSS/trypsin at 1.25% w/v (20 minutes) was used as a positive control. After digestion, samples were embedded in optimal cutting temperature compound (OCT; Sakura Finetek USA, Inc., Torrance, CA), cut into 16 μm axial sections using a Cryostat (Microm HM500, MICROM International GmbH, Waldorf, Germany), and stained with Alcian Blue (AB) to visualize proteoglycan (PG) content. Matrix removal was assessed from diametric sections using ImageJ and normalized to BM controls, where 100% indicates no loss in staining area and 0% indicates a complete removal of staining throughout the sample diameter (n=3/group).

2.4 Fabrication and Characterization of Collagenase-Releasing Nanofibers

Having established a mechanism for entrapping active enzymes, we next fabricated fibers containing a more clinically relevant enzyme, namely collagenase. In initial studies, nanofibers were spun from a solution of 8% w/v PEO in 1:1 EtOH and distilled H_2O with or without 1.25% w/v collagenase. Solutions were spun onto glass cover slips for 10-15 minutes as previously described. To demonstrate retention of collagenase activity, juvenile bovine cartilage samples were prepared as described previously. PEO and PEO-collagenase (PEO-C) nanofibers (0.2 g) were hydrated in BM and the solutions were incubated with cartilage cylinders for 3 and 6 hours, along with BM and BM containing 0.1% w/v collagenase (aqC) controls. Samples were cryotomed and stained with AB and PSR to visualize PG and collagen, respectively (n=4/group). To assess glycosaminoglycan (GAG) loss, % GAG per wet weight was quantified after papain digestion via the 1,9 dimethylmethylene blue (DMMB) assay (n=4/group) [37].

2.5 Scaffold-Mediated Degradation of the Meniscus Interface

Composite scaffolds were fabricated containing 40-50% PEO with the remaining fiber fraction composed of PCL (80 kDa, Sigma-Aldrich). PEO solutions containing 0%, 0.125% (low-dose collagenase, PEO-LC), or 1.25% w/v collagenase (high-dose collagenase, PEO-HC) were electrospun simultaneously with 14.3% w/v PCL in 1:1 tetrahydrofuran and N,N-dimethylformamide (Fisher Scientific, Pittsburgh, PA) onto a common rotating mandrel as previously described [33]. Electrospinning was carried out over 4 hours to form aligned mats approximately 0.5 mm thick, where one jet contained PCL solution and the second jet contained PEO solution with or without collagenase. PEO content was determined by measuring the dry weight of lyophilized scaffolds before and after 24 hours of aqueous submersion on a shaking plate. PEO and PEO-HC solutions were electrospun separately for SEM imaging and fiber diameter measurements (n=100/group) as previously described.

To evaluate the efficacy of these composite scaffolds in providing controlled digestion of the meniscus wound interface, juvenile bovine meniscus bodies were radially sectioned into 10 mm wedges and split horizontally along the inner edge to form a pocket, with two sides remaining intact. Either no scaffold (NS) or a strip of PCL/PEO or PCL/PEO-HC (5 × 10 mm) was inserted into the pocket such that fibers aligned with native collagen architecture. The wound edges were pinned closed with a needle and the samples cultured in BM for either 6 hours or 1, 3, or 7 days (n=3/group). Radial cryotome sections were stained with AB to visualize PG removal from the wound margins. Following this preliminary study, a long-term study with NS, PCL/PEO, PCL/PEO-LC, and PCL/PEO-HC juvenile bovine explant groups was conducted in a chemically-defined medium supplemented with TGF-β3, with culture times of 25 and 50 days (n=8/group). Samples were cryotomed to 16 μm radial sections and stained with either AB or DAPI to visualize PG and nuclei, respectively (n=2/group). The remaining samples were frozen in OCT and the two intact edges removed by a freezing stage sledge microtome. Trimmed samples were glued to sandpaper on a custom grip and extended to failure at 2.5 mm/min using an Instron 5848 Microtester equipped with a 10 N load cell (Instron, Canton, MA). Samples were imaged with a stereoscope after

mechanical testing to quantify the area of potential integration. Integration strength was calculated by dividing the maximum load before failure by the contact surface area between the two tissue segments (n=5-6/group). To determine if collagenase-releasing scaffolds could also improve integration in mature meniscus, cylindrical adult bovine meniscal explants (8 mm diameter × 10 mm height) with a horizontal defect were fitted with a PCL/PEO-LC or PCL/PEO-HC scaffold. In this case, scaffolds were constructed in annular form (8 mm diameter with 5 mm core) to permit tissue-to-tissue contact within the constructs, which were cultured for 7 days before histological processing. Radial paraffin sections were stained with AB or H&E.

2.6 Statistical Analyses

All statistical analyses were done using SYSTAT (Chicago, IL). Experimental group sizes were chosen based on power analysis using preliminary data. Significance was assessed by one or two-way ANOVA with Tukey's HSD post hoc test to make comparisons between groups ($p \leq 0.05$). Data is presented as the mean ± standard deviation.

3. Results

Digestion of the adult meniscus with aqueous collagenase resulted in a marked decrease in matrix density, such that ECM staining more closely resembled that of the fetal meniscus (Fig. 1B). As enzyme dosage was increased, a controllable level of digestion of the wound edge was achieved, as was reflected by the altered μCT signal at the construct edges 1 week after treatment (Fig. 2A). Long-term culture of adult constructs showed improved cellularity and integration with increasing levels of collagenase digestion. By 4 weeks, cells and new collagen fibrils closed approximately 92% of the wound gap in adult HC samples, which exhibited superior integration compared to LC samples (74%) and BM controls (43%) (Figs. 2A and 2B, $p \leq 0.05$). Cell density at the annulus-core boundary was significantly higher for HC samples compared to all other groups, with a 213% and 170% increase over BM controls at 4 and 8 weeks, respectively (Fig. 2C, $p \leq 0.05$). Similarly, total DNA content per dry weight of HC samples was significantly higher than BM controls at 4 and 8 weeks, increasing by 44% and 55%, respectively (Fig. 2D, $p \leq 0.05$). Although LC samples did not show the same level of cellular proliferation relative to HC samples, cell density and total DNA content were significantly higher than BM controls at 8 weeks (Figs. 2C and 2D, $p \leq 0.05$). For both LC and HC groups, total DNA content increased between 4 and 8 weeks by 41 and 38%, respectively, whereas BM controls did not show a significant change in DNA over this time period (Fig. 2D, $p \leq 0.05$).

To facilitate targeted enzyme delivery, PEO nanofibers containing active trypsin or collagenase were fabricated. Nanofibers with and without trypsin were of similar fiber diameter and morphology (200 ± 50 vs. 192 ± 44 nm, $p \geq 0.05$). When cell monolayers were exposed to PEO-trypsin fibers hydrated in HBSS (PEO-T), a dose- and time-dependent change in cell morphology was observed. Cells in PEO-T rounded and lifted from the substrate over a period of 60 minutes, mimicking standard trypsin treatment, though at a much reduced time scale (Fig. 3A). Conversely, there was no apparent change in cell morphology with exposure to hydrated PEO fibers or BM; HBSS alone slightly disrupted monolayer integrity. Cell viability was unaffected by the presence of PEO, as lifted cells reattached after 24 hours upon addition of BM (data not shown). To further characterize the activity of delivered trypsin, cartilage cylinders were exposed to PEO-T solutions. Staining for PG revealed a time-dependent increase in tissue digestion, where exposure for 3 and 6 hours resulted in 52% and 73% PG removal, respectively (Figs. 3B and 3C, $p \leq 0.05$). This pattern and extent of PG removal was comparable to treatment with 1.25% w/v trypsin solution, which showed a 59% removal after 20 minutes of exposure (Fig. 3C, dashed line). There was no change in PG staining for cartilage exposed to BM, HBSS, or PEO fibers.

PEO nanofibers containing active collagenase were produced using a similar approach. While SEM images of fibers with and without collagenase were again comparable in diameter (Fig. 4A, 329 ± 114 vs. 321 ± 135 nm, $p \geq 0.05$), fibers containing enzyme were qualitatively rougher in appearance. To characterize enzyme activity, cartilage cylinders were exposed to PEO-collagenase nanofibers hydrated in BM (PEO-C). PG removal was evident after treatment with either PEO-C or 0.1% w/v aqueous collagenase (aqC) (Fig. 5A). Quantitative analysis of cartilage cylinders showed that exposure to PEO-C for 3 and 6 hours resulted in a 45% and 61% decrease in GAG content compared to exposure to BM, respectively (Fig. 5B, $p \leq 0.05$), and comparable to treatment with aqC (61% at 3 hours, dashed line). PSR staining of collagen increased after digestion due to the better penetration of the stain after GAG removal from the matrix [38].

When collagenase-releasing scaffolds were placed in a juvenile bovine meniscus defect, loss of PG was apparent at the wound edge within 6 hours, with decreased staining intensity persisting through day 7 (Fig. 6B). This loss did not extend to the periphery of treated samples and was not observed in controls, suggesting local action of the enzyme. Long-term culture of these constructs revealed increased tissue porosity and cellularity at the wound edge after collagenase delivery (Fig. 6C). Although the integration strength of all groups remained relatively low at 25 days, by 50 days there was significant improvement for the PCL/PEO and low-dose collagenase scaffold (PCL/PEO-LC) groups (Fig. 6D, $p \leq 0.05$). Meniscal repairs with PCL/PEO-LC scaffolds exhibited the highest integration strength at 50 days (13.5 ± 4.1 kPa), showing a trend toward improvement compared to controls without scaffolds (7.5 ± 3.6 kPa, $p \leq 0.1$). However, integration strength of the high-dose collagenase scaffold (PCL/PEO-HC) group at 50 days (6.9 ± 6.5 kPa, $p \leq 0.05$) was significantly lower than the PCL/PEO-LC group, most likely due to over-digestion of the wound interface. Collagenase-releasing scaffolds placed inside adult meniscal explants also showed evidence of localized digestion and PG loss after 7 days in culture (Fig. 7B). However, the scaffold appeared to inhibit tissue formation at the sample edge in the short-term, and integration was only observed within the fenestrated portion of the annular scaffold (Fig. 7D).

4. Discussion

Orthopaedic injuries involving dense connective tissues are prevalent and suffer from a limited healing capability [3-5]. In the case of the meniscus, treatment success rate declines with age and resulting repair failures frequently culminate in tissue removal to alleviate inflammation and pain [5-7]. However, partial meniscectomy alters joint biomechanics and hastens osteoarthritis [8, 9], prompting the need for novel methods to enhance endogenous repair processes. We hypothesized that decreasing the local ECM density may facilitate meniscal repair and found that the *in vitro* integration of adult meniscus improved after collagenase treatment of the wound boundary. This improvement was accompanied by an initial decrease in local ECM density and an increase in cellularity and matrix synthesis at the interface, supporting our hypothesis. To translate these findings clinically, we developed a delivery system in which active enzyme is stored within water-soluble PEO nanofibers and released into the environment upon hydration. Collagenase-releasing nanofibers, incorporated into a composite scaffold and placed inside a meniscus defect, localized the degradation process to the wound margin and improved tissue integration in a dose-dependent fashion. Given its simplicity and capacity for rapid translation, this innovative approach could aid the many patients who would otherwise undergo meniscus removal.

Repair potential of dense connective tissues declines significantly with age [22-24]. While this is commonly attributed to the hypovascular nature of the tissue as it matures and hence the lack of nutrients and growth factors available for repair [3-5, 21], decreased cellularity

and increased ECM density may also play a role [22, 25]. Although dense aligned collagen bundles are necessary to resist deformation during physiologic loading, this microstructure may also inhibit cell motility and division, thus preventing reparative cells from migrating to the wound site in sufficient numbers. Indeed, fetal repair construct ECM exhibited smaller collagen fibers and had a visibly higher cell density compared to adult constructs (Fig. 1B). Treating the adult constructs with collagenase from *Clostridium histolyticum* cleaved collagen fibrils at the interface and may have increased ECM porosity near the wound edge. Although over-digestion may result in a detrimental loss of structural proteins and cell death [39], restricting digestion to the outermost portion of the wound interface initiated an integrative repair response that was reminiscent of the skeletally immature meniscus.

Global enzymatic treatment has previously been used to stimulate connective tissue repair, most frequently in cartilage-to-cartilage integration studies. Short duration exposure of cartilage constructs to matrix-degrading enzymes increased proliferative cells, ECM synthesis, and integration strength compared to controls [29-31]. Similarly, our partially-digested meniscus constructs had a higher cell density at the interface and greater DNA content than untreated controls. More notably, bridging tissue closed over 90% of the wound gap in HC constructs by 4 weeks, over a two-fold increase compared to BM controls. Tissue filling the wound gap of treated constructs consisted of fine fibrils that did not exhibit birefringence under polarized light, indicative of newly synthesized collagen. In contrast, BM constructs did not produce bridging tissue even when the interface was histologically in contact, making it difficult to determine the extent of true integration in untreated controls. Thus, while matrix synthesis at the wound edge declines with development [40], this trend can be reversed by decreasing the ECM density to a less mature state, although decrease in tissue stiffness [41], removal of matrix PGs [42], and/or presence of collagen fragments [43] may also have contributed to the enhanced repair of digested constructs. Importantly, injectable collagenase is already used to treat Dupuytren's contracture, a fibroproliferative disorder that affects digit mobility [39]. If applied in a targeted and controlled manner, this enzyme may prove beneficial to meniscal injuries as well.

Having established the therapeutic potential of partial digestion for meniscus integrative repair, we next developed a method by which local enzyme delivery to the wound site could be achieved using well-established biomaterials. While the application of electrospun fibers as carriers of biological agents such as antibiotics [44] and growth factors [45, 46] is abundant in the literature, the inclusion of enzymes is not well-documented. A patent by Smith et al. refers to preserving biological materials using fiber-forming techniques and documents the storage of trypsin inside electrospun poly(ethyl oxazoline) [47]. PEO was chosen for our study because of its biocompatibility, solubility in water, and previous use in electrospun composites. In our earlier work, PEO nanofibers were exploited as sacrificial filler in composite PCL/PEO scaffolds, designed to increase porosity and improve cell infiltration [16, 33, 34]. These fibers can be readily functionalized to include bioactive factors or drug-containing microspheres during the electrospinning process, as PEO solutions can be prepared and electrospun from water rather than organic solvents used for other biodegradable polymers [35, 36]. Furthermore, PEO is an ideal delivery system for factors that require a rapid initial release, including the degradative enzymes in our study that are meant to act immediately upon scaffold implantation and denature quickly thereafter to prevent over-digestion. Indeed, our studies show that eluant from trypsin-containing fibers caused cell detachment from plastic substrates within 60 minutes and both trypsin and collagenase released from PEO fibers removed approximately half of the PGs within cartilage cylinders after 3 hours.

To form stable scaffolds with degradative capacity, enzyme-containing PEO nanofibers were electrospun concurrently with PCL to create composites with discrete fiber populations

with differing roles. The aligned PCL fiber fraction acts as a physical template to provide mechanical integrity and instruction for organized ECM synthesis [32]. This may be particularly appropriate when such scaffolds are used to treat horizontal or vertical tears of the meniscus, where the scaffold architecture matches the collagen organization of the native tissue. On the other hand, PEO fibers rapidly dissolve upon hydration to release the embedded collagenase in order to partially degrade the wound interface. A major consequence of PEO fiber removal is an increase in the scaffold pore size, which facilitates cell migration into the regenerate space [16, 33, 34]. However, the scaffolds placed within meniscus defects were not well colonized despite having an initial PEO content of 40-50%, a composition that allowed cell infiltration yet maintained tensile properties in previous studies [33]. It is possible that compression imposed by the defect geometry may have reduced scaffold porosity and as such, the increase in integration likely resulted from the improved matrix synthesis and integration occurring adjacent to the scaffold. In a preliminary study with adult meniscus, the insertion of an annular scaffold that permitted contact of opposing tissue at the center of the construct resulted in rapid bridging matrix formation (Fig. 7). In future studies, additional fenestrations could be introduced to maximize tissue-to-tissue integration.

By using complex scaffolds with multiple components, the fiber ratios, individual fiber properties, and biofactor doses can be tuned to optimize the instructive microenvironment and mechanical properties. For example, composite scaffolds were also utilized by Hong et al. for abdominal laparotomy management, wherein poly(lactide-*co*-glycolide) fibers released an antibiotic and poly(ester urethane) urea provided elasticity [44]. Moreover, fiber modification techniques allow bioactive molecules to be blended inside fibers [44, 45, 47], conjugated to the fiber surface [46], sequestered inside a co-axial core [45], or delivered via microspheres [35]. Consequently, numerous factors can be incorporated into a single scaffold to allow for a multitude of release profiles and therapeutic effects. Building upon this platform, our scaffolds may be further functionalized to include growth factors such as PDGF [15] and TGF-β3 [12] to recruit reparative cells and stimulate ECM synthesis after the initial enzymatic treatment.

5. Conclusions

The principles outlined in this manuscript establish a new approach to enhance repair that recapitulates natural healing processes, including local degradation, cell recruitment, and matrix synthesis. Currently, we are investigating how biomaterial-mediated collagenase delivery impacts *in vivo* meniscal healing in a subcutaneous rat xenotransplant model. For definitive evidence of scaffold efficacy, an ovine model will be used to evaluate integration by inserting the scaffold into a surgically created bucket-handle meniscal defect. Once validated *in vivo*, the nanofibrous networks developed herein, tuned to enhance each phase of fibrous tissue repair, may find widespread application for treating a variety of musculoskeletal tissues.

Acknowledgments

This work was supported by the National Institutes of Health (R01 AR056624 and MSTP T32 GM007170), the Department of Veterans Affairs (I01 RX000174), the Penn Center for Musculoskeletal Disorders, and the Institute for Regenerative Medicine at the University of Pennsylvania. Additional funding was provided by the Musculoskeletal Transplant Foundation, the Armour-Lewis Foundation, and the School of Veterinary Medicine at the University of Pennsylvania. The views expressed in this article are those of the authors and do not necessarily reflect the position or policy of the National Institutes of Health, Department of Veterans Affairs, or the United States government.

8. References

1. Fithian DC, Kelly MA, Mow VC. Material properties and structure-function relationships in the menisci. Clin Orthop Relat Res. 1990; 252:19–31. [PubMed: 2406069]
2. Khetia EA, McKeon BP. Meniscal allografts: biomechanics and techniques. Sports Med Arthrosc. 2007; 15:114–120. [PubMed: 17700370]
3. Makris EA, Hadidi P, Athanasiou KA. The knee meniscus: structure-function, pathophysiology, current repair techniques, and prospects for regeneration. Biomaterials. 2011; 32:7411–31. [PubMed: 21764438]
4. Kawamura S, Lotito K, Rodeo SA. Biomechanics and healing response of the meniscus. Op Tech Sports Med. 2003; 11:68–76.
5. Tu K, Cole BJ, Freedman KB. Augmentation of meniscus repair. Op Tech Sports Med. 2003; 11:127–33.
6. McCarty EC, Marx RG, DeHaven KE. Meniscus repair: considerations in treatment and update of clinical results. Clin Orthop Relat Res. 2002; 402:122–34. [PubMed: 12218477]
7. Rubman MH, Noyes FR, Barber-Westin SD. Arthroscopic repair of meniscal tears that extend into the avascular zone. A review of 198 single and complex tears. Am J Sports Med. 1998; 26:87–95. [PubMed: 9474408]
8. Aagaard H, Verdonk R. Function of the normal meniscus and consequences of meniscal resection. Scand J Med Sci Sports. 1999; 93:134–40. [PubMed: 10380269]
9. Englund M. Meniscal tear--a feature of osteoarthritis. Acta Orthop Scand Suppl. 2004; 75:1–45. [PubMed: 15188684]
10. Zhang Z, Arnold JA, Williams T, McCann B. Repairs by trephination and suturing of longitudinal injuries in the avascular area of the meniscus in goats. Am J Sports Med. 1995; 23:35–41. [PubMed: 7726348]
11. Ochi M, Mochizuki Y, Deie M, Ikuta Y. Augmented meniscal healing with free synovial autografts: an organ culture model. Arch Orthop Trauma Surg. 1996; 115:123–6. [PubMed: 8861574]
12. Ionescu LC, Lee GC, Huang KL, Mauck RL. Growth factor supplementation improves native and engineered meniscus repair in vitro. Acta Biomater. 2012; 8:3687–94. [PubMed: 22698946]
13. Petersen W, et al. The effect of locally applied vascular endothelial growth factor on meniscus healing: gross and histological findings. Arch Orthop Trauma Surg. 2007; 127:235–40. [PubMed: 16896747]
14. Tumia NS, Johnstone AJ. Promoting the proliferative and synthetic activity of knee meniscal fibrochondrocytes using basic fibroblast growth factor in vitro. Am J Sports Med. 2004; 32:915–20. [PubMed: 15150037]
15. Tumia NS, Johnstone AJ. Platelet derived growth factor-AB enhances knee meniscal cell activity in vitro. Knee. 2009; 16:73–6. [PubMed: 18976925]
16. Baker BM, Shah RP, Silverstein AM, Esterhai JL, Burdick JA, Mauck RL. Sacrificial nanofibrous composites provide instruction without impediment and enable functional tissue formation. Proc Natl Acad Sci USA. 2012; 109:14176–81. [PubMed: 22872864]
17. Maher SA, et al. Evaluation of a porous polyurethane scaffold in a partial meniscal defect ovine model. Arthroscopy. 2010; 26:1510–9. [PubMed: 20855181]
18. Pabbruwe MB, Kafienah W, Tarlton JF, Mistry S, Fox DJ, Hollander AP. Repair of meniscal cartilage white zone tears using a stem cell/collagen-scaffold implant. Biomaterials. 2010; 31:2583–91. [PubMed: 20053438]
19. Martinek V, et al. Second generation of meniscus transplantation: in-vivo study with tissue engineered meniscus replacement. Arch Orthop Trauma Surg. 2006; 126:228–34. [PubMed: 16215722]
20. McNulty AL, Moutos FT, Weinberg JB, Guilak F. Enhanced integrative repair of the porcine meniscus in vitro by inhibition of interleukin-1 or tumor necrosis factor alpha. Arthritis Rheum. 2007; 56:3033–42. [PubMed: 17729298]
21. Arnoczky SP, Warren RF. The microvasculatur e of the meniscus and its response to injury. An experimental study in the dog. Am J Sports Med. 1983; 11:131–41. [PubMed: 6688156]

22. Ionescu LC, Lee GC, Garcia GH, Zachry TL, Shah RP, Sennett BJ, Mauck RL. Maturation state-dependent alterations in meniscus integration: implications for scaffold design and tissue engineering. Tissue Eng Part A. 2011; 17:193–204. [PubMed: 20712419]
23. Beredjiklian PK, Favata M, Cartmell JS, Flanagan CL, Crombleholme TM, Soslowsky LJ. Regenerative versus reparative healing in tendon: a study of biomechanical and histological properties in fetal sheep. Ann Biomed Eng. 2003; 31:1143–52. [PubMed: 14649488]
24. Provenzano PP, Hayashi K, Kunz DN, Markel MD, Vanderby R Jr. Healing of subfailure ligament injury: comparison between immature and mature ligaments in a rat model. J Orthop Res. 2002; 20:975–83. [PubMed: 12382962]
25. Clark CR, Ogden JA. Development of the menisci of the human knee joint. Morphological changes and their potential role in childhood meniscal injury. J Bone Joint Surg Am. 1983; 65:538–47. [PubMed: 6833331]
26. Favata M, Beredjiklian PK, Zgonis MH, Beason DP, Crombleholme TM, Jawad AF, Soslowsky LJ. Regenerative properties of fetal sheep tendon are not adversely affected by transplantation into an adult environment. J Orthop Res. 2006; 24:2124–32. [PubMed: 16944473]
27. Klompmaker J, Jansen HW, Veth RP, Nielsen HK, de Groot JH, Pennings AJ. Porous implants for knee joint meniscus reconstruction: a preliminary study on the role of pore sizes in ingrowth and differentiation of fibrocartilage. Clin Mater. 1993; 14:1–11. [PubMed: 10171996]
28. Ehrbar M, et al. Elucidating the role of matrix stiffness in 3D cell migration and remodeling. Biophys J. 2011; 100:284–93. [PubMed: 21244824]
29. van de Breevaart Bravenboer J, In der Maur CD, Bos PK, Feenstra L, Verhaar JA, Weinans H, van Osch GJ. Improved cartilage integration and interfacial strength after enzymatic treatment in a cartilage transplantation model. Arthritis Res Ther. 2004; 6:R469–76. [PubMed: 15380046]
30. Obradovic B, Martin I, Padera RF, Treppo S, Freed LE, Vunjak-Novakovic G. Integration of engineered cartilage. J Orthop Res. 2001; 19:1089–97. [PubMed: 11781010]
31. Janssen LM, In der Maur CD, Bos PK, Hardillo JA, van Osch GJ. Short-duration enzymatic treatment promotes integration of a cartilage graft in a defect. Ann Otol Rhinol Laryngol. 2006; 15:461–8. [PubMed: 16805379]
32. Baker BM, Mauck RL. The effect of nanofiber alignment on the maturation of engineered meniscus constructs. Biomaterials. 2007; 28:1967–77. [PubMed: 17250888]
33. Baker BM, Gee AO, Metter RB, Nathan AS, Marklein RA, Burdick JA, Mauck RL. The potential to improve cell infiltration in composite fiber-aligned electrospun scaffolds by the selective removal of sacrificial fibers. Biomaterials. 2008; 29:2348–58. [PubMed: 18313138]
34. Ionescu, LC.; Mauck, RL. [2012 Sep 20] Porosity and Cell Preseeding Influence Electrospun Scaffold Maturation and Meniscus Integration in Vitro. Tissue Eng Part A. Available from URL: http://www.ncbi.nlm.nih.gov/pubmed/22994398
35. Ionescu LC, Lee GC, Sennett BJ, Burdick JA, Mauck RL. An anisotropic nanofiber/microsphere composite with controlled release of biomolecules for fibrous tissue engineering. Biomaterials. 2010; 31:4113–20. [PubMed: 20149432]
36. Ionescu, LC.; Fisher, MB.; Schenker, ML.; Esterhai, JL.; Mauck, RL. VEGF Delivery from Electrospun Composites Increases Vascular Density In Vivo; Orthopaedic Research Society Annual Meeting; 2012.
37. Farndale RW, Buttle DJ, Barrett AJ. Im proved quantitation and discrimination of sulphated glycosaminoglycans by use of dimethylmethylene blue. Biochim Biophys Acta. 1986; 883:173–7. [PubMed: 3091074]
38. D'Andrea MR. Collagenase predigestion on paraffin sections enhances collagen immunohistochemical detection without distorting tissue morphology. Biotech Histochem. 2004; 79:55–64. [PubMed: 15513707]
39. Syed F, Thomas AN, Singh S, Kolluru V, Emeigh Hart SG, Bayat A. In vitro study of novel collagenase (XIAFLEX(R)) on Dupuytren's disease fibroblasts displays unique drug related properties. PLoS One. 2012; 7:e31430. [PubMed: 22384021]
40. DiMicco MA, Waters SN, Akeson WH, Sah RL. Integrative articular cartilage repair: dependence on developmental stage and collagen metabolism. Osteoarthr Cartil. 2002; 10:218–25. [PubMed: 11869083]

41. Peyton SR, Putnam AJ. Extracellular matrix rigidity governs smooth muscle cell motility in a biphasic fashion. J Cell Physiol. 2005; 204:198–209. [PubMed: 15669099]

42. Natoli RM, Responte DJ, Lu BY, Athanasiou KA. Effects of multiple chondroitinase ABC applications on tissue engineered articular cartilage. J Orthop Res. 2009; 27:949–56. [PubMed: 19123232]

43. Shi L, Ermis R, Garcia A, Telgenhoff D, Aust D. Degradation of human collagen isoforms by Clostridium collagenase and the effects of degradation products on cell migration. Int Wound J. 2010; 7:87–95. [PubMed: 20529148]

44. Hong Y, Fujimoto K, Hashizume R, Guan J, Stankus JJ, Tobita K, Wagner WR. Generating elastic, biodegradable polyurethane/poly(lactide-co-glycolide) fibrous sheets with controlled antibiotic release via two-stream electrospinning. Biomacromolecules. 2008; 9:1200–7. [PubMed: 18318501]

45. Sahoo S, Ang L, Goh J, Toh S. Growth factor delivery through electrospun nanofibers in scaffolds for tissue engineering applications. J Biomed Mater Res A. 2010; 93:1539–50. [PubMed: 20014288]

46. Ye L, et al. Heparin-Conjugated PCL Scaffolds Fabricated by Electrospinning and Loaded with Fibroblast Growth Factor 2. J Biomater Sci Polym Ed. 2011; 22:389–406.

47. Smith, DJ.; Kataphinan, W.; Reneker, DH.; Dabney, S. Preservation of biological materials using fiber-forming techniques. US Patent. No. 6821479. 2004.

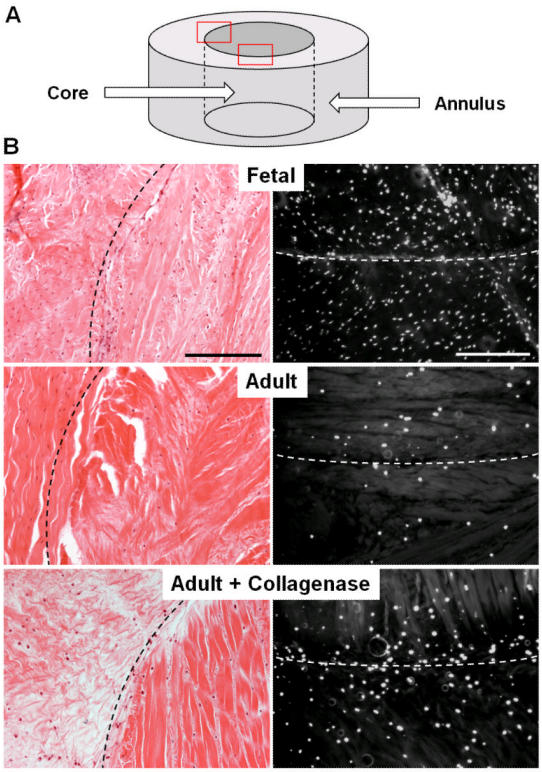

Figure 1.
Aqueous collagenase treatment reduces matrix density and increases cellularity in the adult meniscus, producing a more fetal-like tissue state. (A) Schematic of annulus and core meniscus repair constructs. (B) H&E (left) and DAPI (right) staining of constructs after 4 weeks of culture, where the dashed line indicates the wound interface (n=1-2). Scale = 0.25 mm.

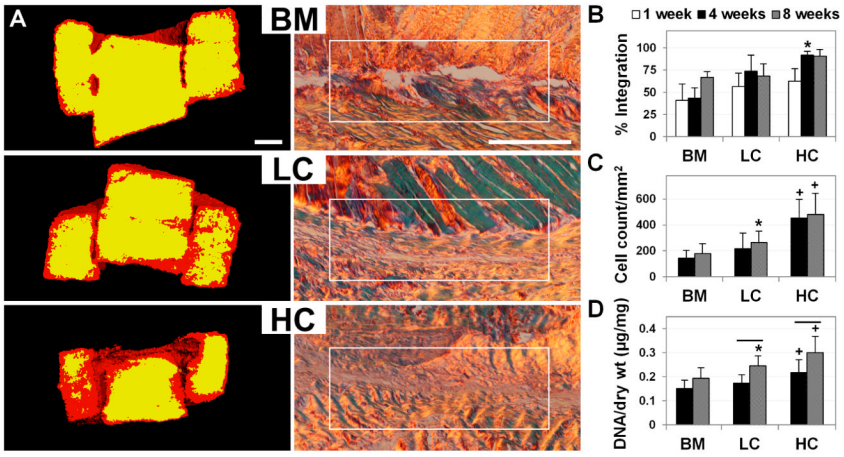

Figure 2.

Improved integration and interface cellularity of adult meniscus after low- (LC) and high-dose (HC) collagenase treatment, compared to controls (BM). (A) Left: 1 week μCT scans showing low (red) and high (yellow) signal intensity correlating to matrix loss at the wound interface (n=4). Scale = 1 mm. Right: 8 week PSR staining of the interface imaged under polarized light showing improved integration with treatment (n=4). Scale = 0.25 mm. (B) Quantification of percent integration normalized to core perimeter (n=3-4), (C) cell density at the interface (n=4), and (D) total DNA content per dry weight (n=6-7). * = $p \leq 0.05$ compared to BM. + = $p \leq 0.05$ compared to BM and LC. Line = $p \leq 0.05$ between 4 and 8 weeks.

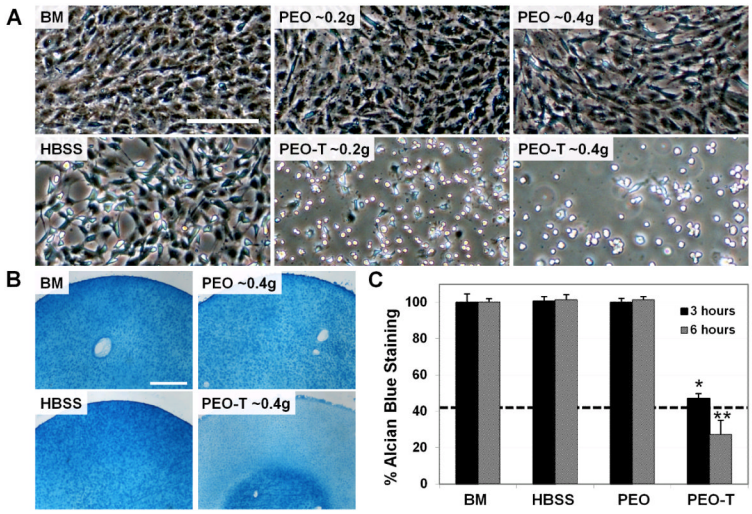

Figure 3.

Sacrificial PEO nanofibers deliver functional enzymes upon hydration. (A) Morphology of cell monolayers treated with eluant from fibers containing trypsin for 60 minutes as a function of fiber mass (n=2). Scale = 0.2 mm. (B) Proteoglycan removal from cartilage cylinders after 6 hours of incubation with BM or HBSS (controls) or eluant from PEO or PEO-T nanofibers (n=3). Scale = 0.5 mm. (C) % AB staining of proteoglycan in cartilage cylinders as a function of treatment group and time, normalized to BM controls (n=3). Dashed line indicates treatment with 1.25% w/v trypsin for 20 minutes as a positive control. * = $p \leq 0.05$ vs. other groups at 3 hours. ** = $p \leq 0.05$ vs. all other groups and time points.

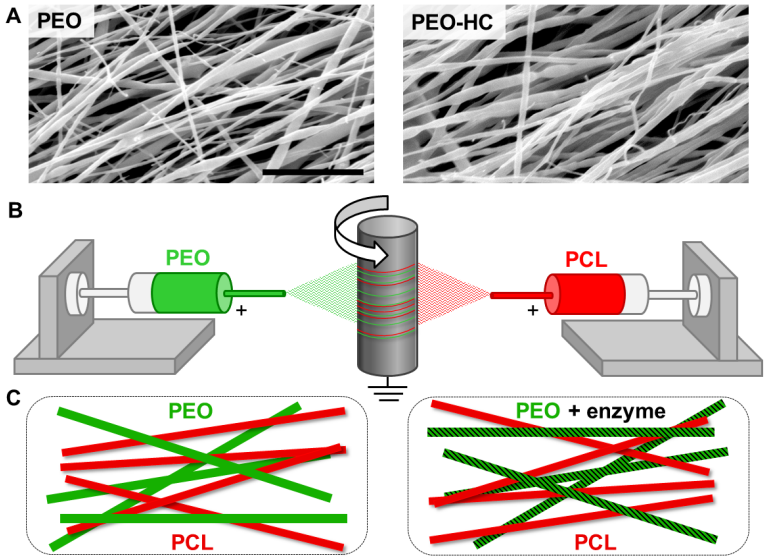

Figure 4.
Fabrication of enzyme-delivering nanofibrous composites. (A) SEM micrographs of PEO (left) and PEO-HC (right) nanofibers. Scale = 5 μm. (B) Schematic of electrospinning setup and (C) composite scaffolds produced with sacrificial PEO fiber fractions that deliver enzyme.

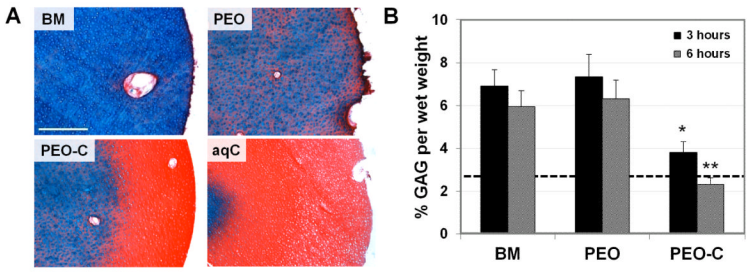

Figure 5.

Release of active collagenase from PEO fibers. (A) Combined AB and PSR staining of cartilage cylinders after 6 hours of exposure to BM, PEO, PEO-C, or aqueous collagenase (aqC, 0.1% w/v) solution (n=4). Scale = 0.5 mm. (B) GAG content of cartilage cylinders as a function of treatment and time (n=4). Dashed line indicates treatment with aqC for 3 hours. * = $p \leq 0.05$ compared to other groups at 3 hours. ** = $p \leq 0.05$ compared to all other groups at 6 hours.

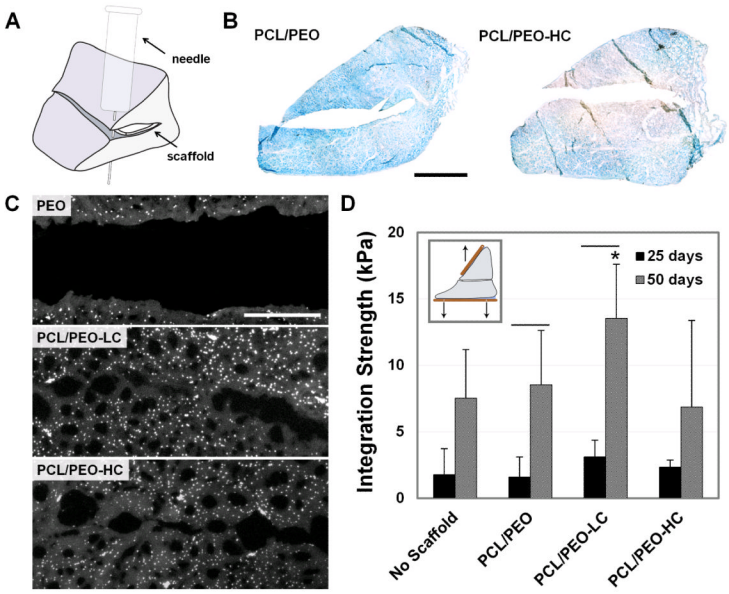

Figure 6.

Integrative repair of juvenile meniscus treated with collagenase-releasing scaffolds. (A) Schematic of repair construct with scaffold placed inside a horizontal meniscal tear. (B) AB staining of meniscus on day 7 with insertion of control and of collagenase-releasing composite scaffolds (n=3). Scale = 5 mm. (C) DAPI staining of wound interface after 50 days of culture with PCL/PEO, PCL/PEO-LC, and PCL/PEO-HC scaffolds (n=2). Scale = 0.25 mm. (D) Integration strength as a function of culture duration. Inset shows mechanical testing setup (n=5-6). * = $p \leq 0.05$ compared to PCL/PEO-HC. Line = $p \leq 0.05$ between 25 and 50 days.

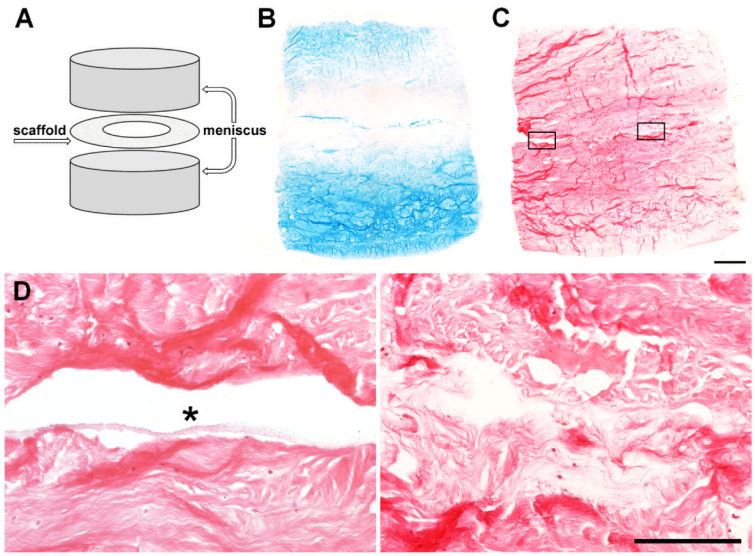

Figure 7.

Improved repair of adult meniscus with collagenase-releasing composite scaffolds. (A) Repair construct schematic with annular scaffold insert. (B) AB and (C) H&E staining of constructs containing annular PCL/PEO-LC scaffolds on day 7. Scale = 1 mm. (D) Magnified areas from (C). Left: lack of integration at the edge occupied by the scaffold (asterisk). Right: bridging tissue in the interior after collagenase delivery. Scale = 0.25 mm.